HEPATOBILIARY-PANCREAS

Hepatobiliary contrast uptake patterns on gadoxetic acid–enhanced MRI in liver metastases from pancreatic ductal adenocarcinoma: can it predict prognosis?

Yoshifumi Noda [1,2] · Toru Tochigi [1,3] · Vinit Baliyan [1] · Hamed Kordbacheh [1] · Avinash Kambadakone [1]

Abstract

Objectives To evaluate the relationship between the patterns of hepatobiliary phase (HBP) contrast uptake in liver metastases on gadoxetic acid–enhanced MR imaging and overall survival (OS) in patients with pancreatic ductal adenocarcinoma (PDAC).

Methods This retrospective study was approved by our institutional review board and written informed consent was waived. A total of 57 patients (30 men and 27 women; age range, 46–92 years; mean age, 64.9 ± 9.2 years) with PDAC and liver metastasis who had undergone gadoxetic acid–enhanced MR imaging were included. The internal morphologies of the nodules were classified as heterogeneous or homogeneous on HBP images (20 min). During patient-by-patient analysis, patients with both patterns of nodules were classified as belonging to the heterogeneous group. Kaplan–Meier analysis and log-rank test were conducted for univariate analysis and Cox proportional hazards regression was conducted for multivariate analysis to evaluate prognostic factors for OS in patients with PDAC and liver metastasis.

Results A total of 199 liver metastases were analyzed, among which 138 nodules (69%) demonstrated heterogeneous hypointensity, while 61 nodules (31%) demonstrated homogeneous hypointensity. Homogeneous hypointense nodules were encountered in 18 patients (32%; homogeneous group), heterogeneous in 29 patients (51%), and both patterns co-existed in 10 patients (17%; heterogeneous group). The heterogeneous group exhibited lower OS rates than the homogeneous group (mean OS, 48.5 months vs 23.9 months; $p = 0.032$).

Conclusions Hepatobiliary contrast uptake pattern in liver metastasis on HBP images can be a potential imaging biomarker to predict OS in patients with PDAC and liver metastasis.

Key Points
• *Majority of the liver metastases were heterogeneous (69%) after gadoxetic acid–enhanced MR imaging.*
• *Patients with heterogeneous hypointense nodules demonstrated lower overall survival rate.*
• *Hepatobiliary contrast uptake pattern in liver metastasis is possibly associated with patients' prognosis.*

Keywords Pancreatic cancer · Metastasis · Magnetic resonance imaging · Contrast agent

✉ Avinash Kambadakone
akambadakone@mgh.harvard.edu

1   Department of Radiology, Massachusetts General Hospital, Harvard Medical School, 55 Fruit Street, White 270, Boston, MA 02114, USA

2   Department of Radiology, Gifu University, 1-1 Yanagido, Gifu 501-1194, Japan

3   Department of Frontier Surgery, Chiba University Graduate School of Medicine, 1-8-1 Inohana, Chuo-ku, Chiba City 260-8670, Japan

Abbreviations

CA	Carbohydrate antigen
CEA	Carcinoembryonic antigen
CNR	Contrast-to-noise ratio
HBP	Hepatobiliary phase
HR	Hazard ratio
MR	Magnetic resonance
OATP	Organic anion transporter proteins
OS	Overall survival
PDAC	Pancreatic ductal adenocarcinoma
SD	Standard deviation
SNR	Signal-to-noise ratio

Introduction

Pancreatic ductal adenocarcinoma (PDAC) is one of the most lethal cancers, with an overall 5-year survival rate of approximately 8.5% [1]. Majority of the patients present with locally advanced disease or metastases due to aggressive tumor biology which contributes to the poor prognosis. Liver is the most common site of distant metastases in PDAC which has been reported in approximately 80% of patients during the later stages of disease [2]. Additionally, 60–70% of patients who undergo curative surgery are bound to develop metastatic disease within 5 years of resection [3].

MR imaging can provide significantly better diagnostic performance for characterizing focal liver lesions [4]. Gadolinium ethoxybenzyl diethylenetriamine pentaacetic acid (Gd-EOB-DTPA, Eovist® or Primovist®, Bayer HealthCare) is a liver-specific contrast material that has been found to be useful for the detection of liver metastases in patients with PDAC [5]. The excellent lesion-to-liver contrast on hepatobiliary phase (HBP) images enables improved sensitivity for detection of liver metastases compared with contrast-enhanced CT especially in small lesion < 10 mm (90% in MRI and 62–64% in CT) [5]. This contrast agent is a substrate for specific hepatocyte membrane transporters known as organic anion transporter proteins (OATP; specifically, 1B3 variant). In principle, non-hepatocyte origin hepatic lesions cannot actively uptake gadoxetic acid; hence, they exhibit hypointensity on HBP images. However, it is interesting to note that, in the recent times, studies have shown that the transporter responsible for gadoxetic acid uptake is expressed in various cancer cells [6]. In fact, liver metastases from colorectal cancer often appear hyperintense on HBP images and the respective patients are often associated with poor prognosis [7]. To the best of our knowledge, there is no previously published study that has evaluated the association between imaging findings of liver metastasis from PDAC and patients' outcome. Therefore, the present study aimed to evaluate the relationship between the patterns of HBP contrast uptake in liver metastases on gadoxetic acid–enhanced magnetic resonance (MR) imaging and overall survival (OS) in patients with PDAC.

Materials and methods

Patients

This retrospective study was approved by our institutional review board, and the need for written informed consent was waived. Between September 2012 and September 2019, 63 consecutive patients with pathologically proven PDAC who underwent gadoxetic acid–enhanced MR imaging and had at least one liver metastasis at presentation of disease were identified. Among them, 6 patients were excluded because of the use of scan parameters different from standard examination ($n = 4$) and respiratory motion artifact ($n = 2$). Consequently, the remaining 57 patients (mean ± standard deviation (SD) age, 64.9 ± 9.2 years; age range, 46–92 years) were included in our study. Overall, 30 patients were men (mean ± SD age, 63.8 ± 10.3 years; range, 46–92 years) and 27 were women (mean ± SD age, 66.1 ± 7.8 years; range, 49–81 years). Out of the 57 patients, 44 patients received chemotherapy or chemoradiation therapy as neoadjuvant ($n = 12$), adjuvant ($n = 4$), or palliative therapy ($n = 28$). Neoadjuvant chemoradiation therapy options were 50.4 Gy/28 fractions of external beam radiation and FOLFIRINOX (a regimen composed of folinic acid, fluorouracil, irinotecan, and oxaliplatin) ($n = 7$), combined gemcitabine and nab-paclitaxel (PTX) ($n = 3$), or capecitabine ($n = 2$). Adjuvant chemotherapy option was gemcitabine ($n = 4$). Palliative chemotherapy options were FOLFIRINOX ($n = 19$) or combined gemcitabine and PTX ($n = 9$).

MR imaging parameters

MR imaging of the pancreas was performed using a 1.5-T (Signa HDxt; GE Healthcare and Magnetom Avanto; Siemens) or 3-T MR system (Discovery MR750; GE Healthcare and Magnetom Trio; Siemens) with a phased array receiver coil covering the upper abdomen. The MR imaging protocol consisted of the following sequences: three-dimensional fat-suppressed axial T1-weighted spoiled gradient-echo imaging, in-phase and opposed-phase T1-weighted axial gradient-recalled-echo imaging, respiratory-triggered two-dimensional fat-suppressed axial T2-weighted fast spin echo imaging, and respiratory-triggered two-dimensional axial diffusion-weighted imaging with a single-shot echo-planar sequence.

Dynamic contrast-enhanced images were obtained with 0.025 mmol gadolinium (Gd)/kg body weight for Gd-EOB-DTPA (0.25 mmol Gd/mL; Eovist®, Bayer HealthCare) using T1-weighted fat-suppressed sequences (TR/TE, 3.74/1.82 ms; flip angle, 12°; section thickness, 5 mm; slice gap, 0 mm; field of view, 312 × 400 mm; matrix, 256 × 154; slice number, 44 slices; and acquisition time, 20 s with breath holding): precontrast, arterial dominant phase (35–40 s), portal venous phase (60–75 s), late phase (3 min), and HBP (20 min) images. Gadoxetic acid was administered intravenously by automatic power injector at a rate of 1 mL/s followed by 20 mL saline flash with the same rate.

Reference standard of liver metastases

In patients with numerous liver metastases, we counted and evaluated liver metastases up to 10 lesions per each patient. Overall, 344 liver metastases were identified in 57 patients. Among them, 145 lesions were excluded from this study because the tumor size was too small (< 5 mm) to perform image

analysis. Pathological confirmation was obtained by CT-guided biopsy ($n = 19$) or surgical resection/partial hepatectomy ($n = 4$). In the remaining 34 patients, confirmation of metastases was obtained based on a combination of typical imaging findings, clinical picture, and increase in size of the lesions on follow-up images. The typical imaging findings used for diagnosis of metastases included hyperintensity on T2-weighted imaging, restricted diffusion and hypoenhancement on dynamic early post-gadolinium-enhanced images, and hypointensity on HBP images.

Qualitative image analysis

Qualitative image analysis was performed by two independent readers (Y.N. and T.T.; 8 and 12 years of post-training experience in interpreting abdominal MR images, respectively) on PACS (AGFA IMPAX Viewer). The readers evaluated the HBP images acquired 20 min after injection with contrast agent [8]. The readers were blinded to patients' clinical information or outcomes. Consequently, the patterns of HBP contrast uptake in liver metastases were evaluated and each nodule was classified as homogeneous or heterogeneous hypointense in consensus. Homogeneity was defined as a signal intensity that was similar to or lower than that of the inferior vena cava, whereas heterogeneity was when the signal intensity was higher than that of the inferior vena cava with areas of internal heterogeneity. During patient-by-patient analysis, patients with only homogeneous hypointense nodules were placed in the homogenous group, whereas patients with only heterogeneous hypointense nodules or both patterns of nodules were placed in the heterogeneous group.

Quantitative image analysis

Quantitative assessment of the liver metastases was performed by quantifying the signal intensities of liver metastasis (SI_{nodule}) and liver parenchyma (SI_{liver}) on the HBP images by carefully excluding vessels and bile ducts. The background noise was quantified as the SD of the signal intensity of the liver parenchyma (SD_{liver}), whereas the signal-to-noise ratio (SNR) of the liver metastasis was calculated as a ratio of the liver metastasis signal intensity to the background noise. Furthermore, the tumor-to-liver contrast-to-noise ratio (CNR) was calculated using the following equation: $CNR = (SI_{liver} - SI_{nodule}) / SD_{liver}$. Additionally, the maximum diameter of liver metastasis was measured on HBP axial or coronal images with greatest dimension.

Statistical analysis

Statistical analyses were performed using the MedCalc version 19.1.3 software program for Windows (MedCalc Software). The Mann–Whitney U and Fisher exact tests were conducted to compare patients' age, sex, presence or absence of chemotherapy, plasma carcinoembryonic antigen (CEA) and carbohydrate antigen (CA) 19-9 levels, number of liver metastases, and presence or absence of extrahepatic metastasis between homogeneous and heterogeneous groups. The Mann–Whitney U test was conducted to compare maximum diameter of liver metastasis, SNR, and CNR between homogeneous and heterogeneous hypointense nodules. Kaplan–Meier analysis and log-rank test were conducted for univariate analysis and Cox proportional hazards regression was conducted for multivariate analysis to evaluate prognostic factors for OS in patients with PDAC and liver metastasis. To assess interobserver variability in the definitions for the homogeneous and heterogeneous groups, κ statistics was used to measure the degree of interobserver agreement. A p value < 0.05 was considered to be statistically significant.

Results

Patient demographics and tumor characteristics

Patient demographics and tumor characteristics are summarized in Tables 1 and 2. The mean follow-up interval for the 57 patients included in this study was 15.3 months (range, 0.1–61.3 months) following the diagnosis of liver metastasis. During the follow-up period, 23 patients died with an estimated 5-year survival rate of 20.1% and the mean survival time of 29.9 months.

Qualitative assessment of enhancement on hepatobiliary phase images

Majority of the nodules ($n = 138$, 69%) demonstrate heterogeneous hypointensity, while nearly a third of metastatic nodules were homogeneous ($n = 61$, 31%). Homogeneous and heterogeneous hypointense nodules were encountered in 18 (32%) and 29 (51%) patients, respectively, and both patterns coexisted in 10 patients (17%). Patients were further classified into homogeneous (18 patients) and heterogeneous (39 patients) groups (Fig. 1).

The number of liver metastases was significantly greater in the heterogeneous group than in the homogeneous group (5.5 ± 3.8 vs 2.7 ± 2.3, $p = 0.015$). Although no significant difference was found in patients' age, sex, presence or absence of chemotherapy, plasma CEA and CA 19-9 levels, and presence or absence of extrahepatic metastasis ($p = 0.13$–0.90), tumor markers tended to be higher in the heterogeneous group than in the homogeneous group (Table 1). The sites of extrahepatic metastasis which were confirmed by follow-up imaging included the lung ($n = 13$), peritoneal carcinomatosis ($n = 7$), bone ($n = 5$), lymph node ($n = 2$), adrenal gland ($n = 2$), cerebellum ($n = 1$), and kidney ($n = 1$).

Table 1 Background factors between homogeneous and heterogeneous groups

	Homogeneous group	Heterogeneous group	*p* value
Number of patients	18	39	N.A.
Age (year)	66.9 ± 9.8 (46–81)	63.9 ± 8.8 (47–92)	0.13
Gender (M:F)	8:10	22:17	0.57
Chemotherapy (presence:absence)	16:2	28:11	0.19
CEA (ng/mL)	9.2 ± 13.7 (0.9–51.7)	18.4 ± 33.3 (1.0–157.0)	0.90
CA 19-9 (U/mL)	4587.6 ± 9033.3 (1.0–28,555.0)	18,706.0 ± 93,881.4 (1.0–563,681.0)	0.45
Number of liver metastasis	2.7 ± 2.3 (1–> 10)	5.5 ± 3.8 (1–> 10)	0.015*
Extrahepatic metastasis (presence:absence)	10:8	24:15	0.77

N.A. not applicable, *CEA* carcinoembryonic antigen, *CA 19-9* carbohydrate antigen 19-9

*$p < 0.05$, significant difference

Quantitative assessment

The maximum diameter of liver metastasis ($p = 0.0001$) and SNR ($p < 0.0001$) were significantly greater in the heterogeneous hypointense nodules than in the homogeneous ones. The CNR was significantly greater in the homogeneous hypointense nodules than in the heterogeneous ones ($p = 0.0016$) (Table 2). For Kaplan–Meier method and log-rank test, patients were classified into two groups using median values of age (64.0 years), maximal diameter of liver metastasis (11.5 mm), and number of liver metastasis (3 lesions). Plasma CEA (5.0 ng/mL) and CA 19-9 (37.0 U/mL) cutoff values were based on our institutional standard.

Patient outcome

Table 3 demonstrates the results of univariate and multivariate analyses of prognostic factors for OS. For Kaplan–Meier method and log-rank test, patients were classified into two groups using median values of age (64.0 years), maximum diameter of liver metastasis (11.5 mm), and number of liver metastasis (3 lesions). Plasma CEA (5.0 ng/mL) and CA 19-9 (37.0 U/mL) cutoff values were based on our institutional standard. Significant prognostic factors for OS in multivariate analysis were as follows: maximum diameter of liver

metastasis (hazard ratio (HR): 0.92; $p = 0.037$) and pattern of HBP contrast uptake (HR: 4.66; $p = 0.018$). The heterogeneous group had lower OS compared with the homogeneous group (mean OS, 48.5 months vs 23.9 months; $p = 0.032$) (Figs. 2, 3, and 4).

Discussion

In principle, liver metastases do not exhibit any uptake of hepatobiliary contrast agent on the HBP images and therefore remain hypointense [9]. However, several radiologic studies have described atypical or paradoxical uptake of gadoxetic acid in liver metastases on HBP [9–11]. Throughout our clinical experience, we have also observed paradoxical uptake in liver metastases on HBP images in patients with PDAC. To our knowledge, there are limited data on the relationship between the patterns of HBP contrast uptake by liver metastases and patient outcomes. Our study demonstrated that patients with PDAC who present heterogeneous hypointense liver metastasis on HBP images are associated with lower OS rate than patients with homogeneous hypointense nodules.

Gadoxetic acid is a liver-specific MR imaging contrast agent that is taken into hepatocytes by a transporter OATP1B3. Consequently, liver parenchyma and

Table 2 Tumor characteristics

	Homogeneous hypointense nodule	Heterogeneous hypointense nodule	*p* value
Number of lesions	61	138	N.A.
Maximum diameter (mm)	11.7 ± 10.6 (5.0–76.9)	15.7 ± 10.9 (5.0–70.0)	0.0001*
SNR	8.9 ± 3.6 (2.3–18.7)	13.5 ± 5.4 (3.6–25.8)	< 0.0001*
CNR	15.2 ± 5.2 (5.2–28.4)	12.8 ± 6.3 (1.6–28.9)	0.0016*

N.A. not applicable, *SNR* signal-to-noise ratio, *CNR* tumor-to-liver contrast-to-noise ratio

*$p < 0.05$, significant difference

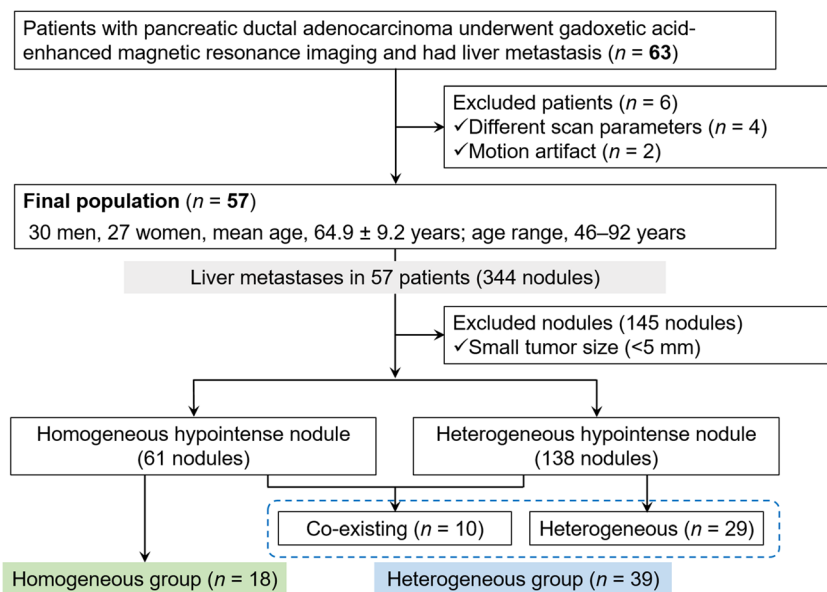**Fig. 1** Flow chart showing included and excluded patients

Table 3 Univariate and multivariate analyses for prediction of overall survival

Prognostic factors	Univariate analysis		Multivariate analysis	
	Hazard ratio	p value	Hazard ratio	p value
Age		0.51		
≤ 64.0 years	1			
> 64.0 years	1.32			
Gender		0.73		
Male	1			
Female	1.15			
Chemotherapy		0.58		
Absence	1			
Presence	0.73			
CEA		0.80		
≤ 5 ng/mL	1			
> 5 ng/mL	1.13			
CA 19-9		0.11		
≤ 37 U/mL	1			
> 37 U/mL	0.45			
Maximal diameter		0.086	0.92	0.037*
≤ 11.5 mm	1			
> 11.5 mm	0.48			
Number of liver metastasis		0.63		
≤ 3	1			
> 3	1.23			
Pattern of HBP contrast uptake		0.032*	4.66	0.018*
Homogeneous	1			
Heterogeneous	2.59			

N.A. not applicable, *CEA* carcinoembryonic antigen, *CA 19-9* carbohydrate antigen 19-9, *HBP* hepatobiliary phase
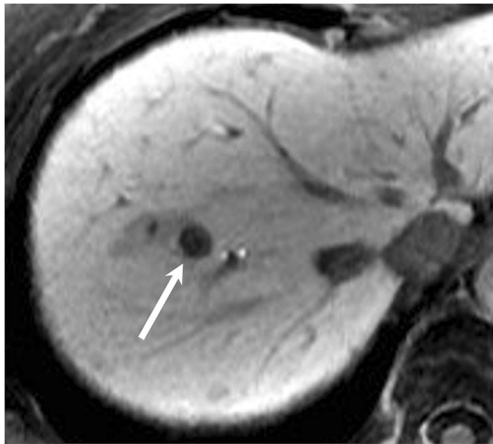
*$p < 0.05$, significant difference

Fig. 2 A 73-year-old female with liver metastases. The axial hepatobiliary phase image at 20 min demonstrates the homogeneous hypointense nodule (arrow) with homogeneous hypointensity. The SNR and CNR were 7.0 and 10.2, respectively. The survival duration was 43.2 months

Fig. 4 Kaplan–Meier overall survival (OS) curves for patients with homogeneous and heterogeneous groups. The heterogeneous group exhibited lower OS rate than the homogeneous group (mean OS, 48.5 months vs 23.9 months; $p = 0.032$)

hepatocellular carcinomas or adenomas of hepatocyte origin typically show enhancement on HBP images [12, 13]. Tumors of non-hepatocyte origin, including liver metastases from PDAC, do not express OATP1B3; therefore, they do not exhibit any uptake of gadoxetic acid and appear hypointense on HBP images [14]. However, aberrant OATP1B3 expression has been confirmed in several tumors of non-hepatocyte origin, including colon cancer, breast cancer, and PDAC [15–19]. Heterogeneous hypointense liver metastases from colorectal cancer or breast cancer have been associated with a worse prognosis or therapeutic response to chemotherapy than that observed in homogeneous hypointense metastases [7, 19]. Immunochemical OATP1B3 overexpression has also been correlated to a worse progression-free survival rate than negative OATP1B3 expression [20]. The aberrant OATP1B3
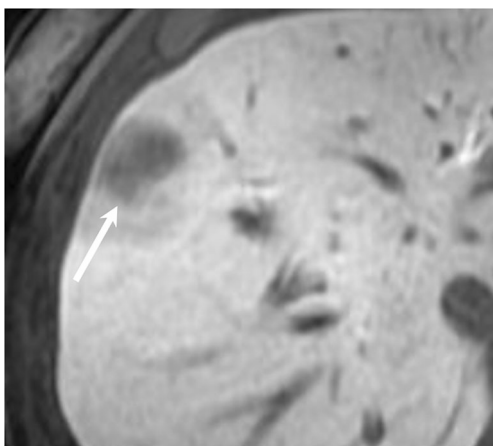

Fig. 3 A 64-year-old female with liver metastases. The axial hepatobiliary phase image demonstrates the heterogeneous hypointense nodule (arrow) with clustered uptake of hepatobiliary contrast agent in the lesion. The SNR and CNR were 15.0 and 8.4, respectively. The survival duration was 9.4 months
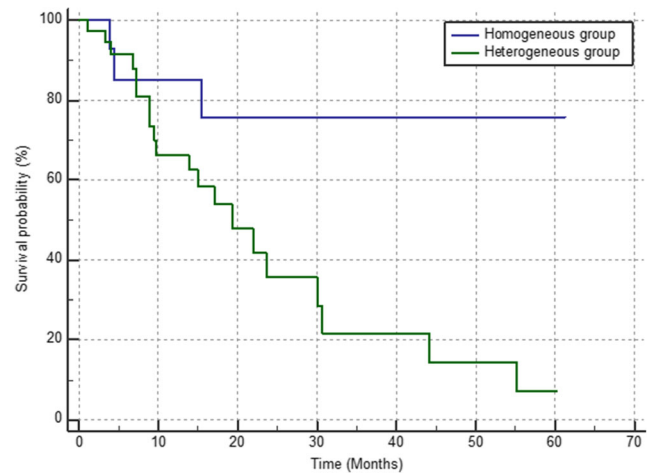
overexpression is associated with decreased apoptosis following chemotherapy and to a significantly more aggressive tumor behavior [15].

Treatment paradigm for PDAC has been changing and early identification of biomarkers for predicting aggressive tumor biology allows dictating treatment strategies. Due to recent effective chemotherapy like FOLFORINOX, patients with locally advanced PDAC and synchronous liver metastasis have a chance to receive subsequent curative surgery [21, 22]. Therefore, in patients with oligometastatic liver disease, identification of pattern of enhancement might allow selection of patients for surgical resection, thereby improving outcome since pancreatic surgeries are not trivial.

Currently, there are no studies that have investigated the relationship between the patterns of HBP contrast uptake in liver metastases on gadoxetic acid–enhanced MR imaging and prognosis in patients with PDAC. However, both colon cancer and PDAC cells have been shown to express aberrant OATP1B3 different from wild-type OATP1B3 expressed in the normal hepatocytes [17]. This aberrant OATP1B3 has only limited transport activity and different subcellular localizations. Although it is necessary to further investigate the biological and clinical significance of the aberrant OATP1B3 expression in PDAC, we believe that OATP1B3 overexpression, which appears as heterogeneous hypointense nodule, is associated with a worse prognosis than negative OATP1B3 expression.

Our study has several limitations. First, we used a retrospective design and performed our study at a single center with a relatively small sample size. Second, pathological evidence was not obtained in all patients. However, there was imaging and clinical confirmation of liver metastases in all patients. Finally, we used various MRI scanners from different manufacturers because of the fact that the study period was

relatively long (84 months). Nonetheless, the liver imaging protocol was standardized particularly with respect to the slice thickness and the phase of acquisition. Further prospective clinical studies including the evaluation of immunochemical OATP1B3 expression are needed to validate our results.

In conclusion, patients with heterogeneous hypointense liver metastases exhibited worse prognosis than those presenting homogeneous hypointense nodules. Hepatobiliary contrast uptake pattern in liver metastasis on HBP images was possibly associated with OS in patients with PDAC and liver metastasis.

Compliance with ethical standards

Guarantor The scientific guarantor of this publication is Avinash Kambadakone.

Conflict of interest AK: Grant support for research activities from Philips and GE Healthcare. Other authors report no relevant disclosures or conflicts of interest.

Informed consent Written informed consent was waived.

Ethical approval Institutional Review Board approval was obtained.

Methodology
• Retrospective
• Diagnostic or prognostic study
• Performed at one institution

References

1. Duggan MA, Anderson WF, Altekruse S, Penberthy L, Sherman ME (2016) The Surveillance, Epidemiology, and End Results (SEER) program and pathology: toward strengthening the critical relationship. Am J Surg Pathol 40:e94–e102
2. Iacobuzio-Donahue CA, Fu B, Yachida S et al (2009) DPC4 gene status of the primary carcinoma correlates with patterns of failure in patients with pancreatic cancer. J Clin Oncol 27:1806–1813
3. DiMagno EP, Reber HA, Tempero MA (1999) AGA technical review on the epidemiology, diagnosis, and treatment of pancreatic ductal adenocarcinoma. American Gastroenterological Association. Gastroenterology 117:1464–1484
4. Jeon SK, Lee JM, Joo I et al (2018) Magnetic resonance with diffusion-weighted imaging improves assessment of focal liver lesions in patients with potentially resectable pancreatic cancer on CT. Eur Radiol 28:3484–3493
5. Motosugi U, Ichikawa T, Morisaka H et al (2011) Detection of pancreatic carcinoma and liver metastases with gadoxetic acid-enhanced MR imaging: comparison with contrast-enhanced multidetector row CT. Radiology 260:446–453
6. Buxhofer-Ausch V, Secky L, Wlcek K et al (2013) Tumor-specific expression of organic anion-transporting polypeptides: transporters as novel targets for cancer therapy. J Drug Deliv 2013:863539
7. Park SH, Kim H, Kim EK et al (2017) Aberrant expression of OATP1B3 in colorectal cancer liver metastases and its clinical implication on gadoxetic acid-enhanced MRI. Oncotarget 8:71012–71023
8. Radiology ACo (2018) Liver Imaging Reporting and Data System version 2018 Manual
9. Campos JT, Sirlin CB, Choi JY (2012) Focal hepatic lesions in Gd-EOB-DTPA enhanced MRI: the atlas. Insights Imaging 3:451–474
10. Ha S, Lee CH, Kim BH et al (2012) Paradoxical uptake of Gd-EOB-DTPA on the hepatobiliary phase in the evaluation of hepatic metastasis from breast cancer: is the "target sign" a common finding? Magn Reson Imaging 30:1083–1090
11. Granata V, Catalano O, Fusco R et al (2015) The target sign in colorectal liver metastases: an atypical Gd-EOB-DTPA "uptake" on the hepatobiliary phase of MR imaging. Abdom Imaging 40:2364–2371
12. Ba-Ssalamah A, Antunes C, Feier D et al (2015) Morphologic and molecular features of hepatocellular adenoma with gadoxetic acid-enhanced MR imaging. Radiology 277:104–113
13. Yamashita T, Kitao A, Matsui O et al (2014) Gd-EOB-DTPA-enhanced magnetic resonance imaging and alpha-fetoprotein predict prognosis of early-stage hepatocellular carcinoma. Hepatology 60:1674–1685
14. Ringe KI, Husarik DB, Sirlin CB, Merkle EM (2010) Gadoxetate disodium-enhanced MRI of the liver: part 1, protocol optimization and lesion appearance in the noncirrhotic liver. AJR Am J Roentgenol 195:13–28
15. Lee W, Belkhiri A, Lockhart AC et al (2008) Overexpression of OATP1B3 confers apoptotic resistance in colon cancer. Cancer Res 68:10315–10323
16. Muto M, Onogawa T, Suzuki T et al (2007) Human liver-specific organic anion transporter-2 is a potent prognostic factor for human breast carcinoma. Cancer Sci 98:1570–1576
17. Thakkar N, Kim K, Jang ER et al (2013) A cancer-specific variant of the SLCO1B3 gene encodes a novel human organic anion transporting polypeptide 1B3 (OATP1B3) localized mainly in the cytoplasm of colon and pancreatic cancer cells. Mol Pharm 10:406–416
18. Murata S, Matsushima S, Sato Y et al (2018) Predicting chemotherapeutic response for colorectal liver metastases using relative tumor enhancement of gadoxetic acid disodium-enhanced magnetic resonance imaging. Abdom Radiol (NY) 43:3301–3306
19. Lee HJ, Lee CH, Kim JW, Park YS, Lee J, Kim KA (2017) Use of hepatobiliary phase images in Gd-EOB-DTPA-enhanced MRI of breast cancer hepatic metastasis to predict response to chemotherapy. Clin Imaging 43:127–131
20. Teft WA, Welch S, Lenehan J et al (2015) OATP1B1 and tumour OATP1B3 modulate exposure, toxicity, and survival after irinotecan-based chemotherapy. Br J Cancer 112:857–865
21. Crippa S, Bittoni A, Sebastiani E et al (2016) Is there a role for surgical resection in patients with pancreatic cancer with liver metastases responding to chemotherapy? Eur J Surg Oncol 42:1533–1539
22. Kartalis N (2018) CT and MRI of pancreatic cancer: there is no rose without a thorn! Eur Radiol 28:3482–3483